



THE UNIVERSITY *of* EDINBURGH

## Edinburgh Research Explorer

### Human AdV-20-42-42, a promising novel adenoviral vector for gene therapy and vaccine product development

**Citation for published version:**

Ballmann, MZ, Raus, S, Engelhart, R, Kaján, GL, Beqqali, A, Hadoke, PW, Van Der Zalm, C, Papp, T, John, L, Khan, S, Boedhoe, S, Danskog, K, Frängsmyr, L, Custers, J, Bakker, WAM, Van Der Schaar, HM, Arnberg, N, Lemckert, AAC, Havenga, M & Baker, AH 2021, 'Human AdV-20-42-42, a promising novel adenoviral vector for gene therapy and vaccine product development', *Journal of Virology*.  
<https://doi.org/10.1128/JVI.00387-21>

**Digital Object Identifier (DOI):**

[10.1128/JVI.00387-21](https://doi.org/10.1128/JVI.00387-21)

**Link:**

[Link to publication record in Edinburgh Research Explorer](#)

**Document Version:**

Version created as part of publication process; publisher's layout; not normally made publicly available

**Published In:**

Journal of Virology

**General rights**

Copyright for the publications made accessible via the Edinburgh Research Explorer is retained by the author(s) and / or other copyright owners and it is a condition of accessing these publications that users recognise and abide by the legal requirements associated with these rights.

**Take down policy**

The University of Edinburgh has made every reasonable effort to ensure that Edinburgh Research Explorer content complies with UK legislation. If you believe that the public display of this file breaches copyright please contact [openaccess@ed.ac.uk](mailto:openaccess@ed.ac.uk) providing details, and we will remove access to the work immediately and investigate your claim.



1       **Human AdV-20-42-42, a promising novel adenoviral vector for gene**  
2                               **therapy and vaccine product development**

3  
4   Mónika Z. Ballmann<sup>1</sup>, Svjetlana Raus<sup>2,#</sup>, Ruben Engelhart<sup>1,2</sup>, Győző L. Kaján<sup>3,\*</sup>, Abdelaziz  
5   Beqqali<sup>2</sup>, Patrick WF Hadoke<sup>2</sup>, Chantal van der Zalm<sup>1</sup>, Tibor Papp<sup>4,\*</sup>, Lijo John<sup>3,+</sup>, Selina  
6   Khan<sup>4</sup>, Satish Boedhoe<sup>4</sup>, Katarina Danskog<sup>3</sup>, Lars Frängsmyr<sup>3</sup>, Jerome Custers<sup>4</sup>, Wilfried  
7   A.M. Bakker<sup>1</sup>, Hilde M. van der Schaar<sup>1</sup>, Niklas Arnberg<sup>3</sup>, Angelique A.C. Lemckert<sup>1</sup>,  
8   Menzo Havenga<sup>1</sup>, Andrew H. Baker<sup>2</sup>

9  
10   **Affiliations:**

11   <sup>1</sup>Batavia Biosciences B.V., Leiden, The Netherlands

12   <sup>2</sup>Centre for Cardiovascular Sciences, University of Edinburgh, Little France Crescent,  
13   Edinburgh, UK

14   <sup>3</sup>Department of Clinical Microbiology, Division of Virology, Umeå University, Sweden

15   <sup>4</sup>Janssen Vaccines and Prevention B.V., Leiden, The Netherlands

16  
17   <sup>#</sup>Present address: Department of Medicine, Division of Hepatology, Albert Einstein College  
18   of Medicine, Bronx, New York

19   <sup>\*</sup>Present address: Institute for Veterinary Medical Research, Budapest, Hungary

20   <sup>+</sup>Present address: National Veterinary Institute, Uppsala, Sweden

21  
22   **Running title:** A novel adenoviral vector for product development

23  
24   **Keywords:** Novel adenovirus type candidate; Expression vector, Low seroprevalence; Cell  
25   and tissue transduction, Potent T-cell responses

26 **Corresponding author:**

27 Andrew H. Baker

28 Centre for Cardiovascular Sciences, University of Edinburgh,

29 Little France Crescent, Edinburgh, UK

30 E-mail : [Andy.Baker@ed.ac.uk](mailto:Andy.Baker@ed.ac.uk)

31 **ABSTRACT**

32 Pre-existing immune responses towards adenoviral vector limit the use of a vector based on  
33 particular serotypes and its clinical applicability for gene therapy and/or vaccination.  
34 Therefore, there is a significant interest to vectorize novel adenoviral types that have low  
35 seroprevalence in the human population. Here, we describe the discovery and vectorization of  
36 a chimeric human adenovirus, which we call HAdV-20-42-42. Full genome sequencing  
37 revealed that this virus is closely related to human serotype 42, except for the penton-base  
38 which is derived from serotype 20. The HAdV-20-42-42 vector could be propagated stably to  
39 high titers on existing E1-complementing packaging cell lines. Receptor binding studies  
40 revealed that the vector utilized both CAR and CD46 as receptors for cell entry. Furthermore,  
41 the HAdV-20-42-42 vector was potent in transducing human and murine cardiovascular cells  
42 and tissues, irrespective of the presence of blood coagulation factor X. *In vivo*  
43 characterizations demonstrate that when delivered intravenously (i.v.) in mice, HAdV-20-42-  
44 42 mainly targeted the lungs, liver and spleen and triggered robust inflammatory immune  
45 response. Finally, we demonstrate that potent T-cell responses against vector-delivered  
46 antigens could be induced upon intramuscular vaccination in mice. In summary, from the  
47 data obtained we conclude that HAdV-20-42-42 provides a valuable addition to the portfolio  
48 of adenoviral vectors available to develop efficacious products in the fields of gene therapy  
49 and vaccination.

50

51 **IMPORTANCE**

52 Adenoviral vectors are currently under investigation for a broad range of therapeutic  
53 indications in diverse fields, such as oncology and gene therapy, as well as for vaccination  
54 both for human and veterinary use. A wealth of data shows that pre-existing immune

55 responses may limit the use of a vector. Particularly in the current climate of global  
56 pandemic, there is a need to expand the toolbox with novel adenoviral vectors for vaccine  
57 development. Our data demonstrates that we have successfully vectorized a novel adenovirus  
58 type candidate with low seroprevalence. The cell transduction data and antigen-specific  
59 immune responses induced *in vivo* demonstrate that this vector is highly promising for the  
60 development of gene therapy and vaccine products.

## 61 INTRODUCTION

62 Adenoviral vectors have been studied for decades as they hold great promise as tools to  
63 develop safe and effective gene therapy and vaccine products. As such, there are dozens of  
64 therapeutic applications being pursued utilizing adenoviral vectors. As it has been amply  
65 demonstrated that host immune responses limit the repeated use of a particular vector (1-4)  
66 there is a constant demand to identify new adenovirus (AdV) serotypes with low  
67 seroprevalence, and alternate tropism. Thus, investigations into the *in vitro* and *in vivo*  
68 biology of less prevalent adenovirus may advance the clinical use of alternative Ad-based  
69 platforms.

70 To date, 104 human adenovirus (HAdV) types have been described and are sub-  
71 grouped in 7 species (HAdV-A-G), of which HAdV-D is the largest. It has been well-  
72 documented that the members of the different species are associated with diverse clinical  
73 symptoms, including gastroenteritis (HAdV-F and -G), respiratory disease (HAdV-B, C, and  
74 E), or conjunctivitis and/or keratitis (HAdV-B and -D). HAdV-induced symptoms can either  
75 be self-limiting and cleared by a host within days to weeks, but persistent infection of HAdV-  
76 C can last for months. Serotype classification is historically based on the unique  
77 neutralization profile of an adenovirus, i.e. serum specifically raised against one serotype  
78 does not cross-neutralize other adenovirus serotypes, and a hemagglutination profile. Besides  
79 the 57 acknowledged serotypes, many hybrid adenoviruses have been discovered and as these  
80 so-called chimeras can be neutralized by parental serum they do not qualify as distinct  
81 serotypes. Most likely such hybrids originate from homologous recombination events  
82 between two or more viruses replicating simultaneously in a host cell during co-infection (5-  
83 8).

84 In the present study we describe the generation of a novel replication-incompetent  
85 vector based on a natural hybrid that we named HAdV-20-42-42. The recombinant HAdV-

86 20-42-42 vector was used for characterization of its seroprevalence, receptor usage, and  
87 tropism. In addition, we explored the utility of the vector as a potential tool to develop gene  
88 therapy and vaccine products. The data obtained and described here warrant further studies  
89 into the utilization of the HAdV-20-42-42 vector to develop vaccines and cardiovascular  
90 intervention strategies.

## 91 RESULTS

### 92 Identification of HAdV-20-42-42, a natural chimera

93 In order to identify possible new vector candidates, e.g. new and/or rare human adenovirus  
94 types, 281 human adenovirus strains isolated from patients in Sweden between 1978 and  
95 2010 were screened previously (9). From these samples, the hexon, the penton base, and the  
96 polymerase genes were amplified and sequenced to allow for identification of new  
97 adenovirus types or possible recombinants. Strains with promising genotypes were  
98 propagated on A549 cells, after which the complete viral genome was sequenced using Next-  
99 Generation Sequencing and annotated based on HAdV reference strains. Phylogenetic  
100 analyses were conducted based on the complete genome sequence and amino acid  
101 translations of the hexon, penton base, and the fiber knob.

102 During the screening process, strain 212 was pinpointed and analyzed further. The  
103 complete genome sequence of this strain was 35,187 bp long with a GC-content of 57.0%. A  
104 typical HAdV-D genome layout was observed with 37 protein coding sequences and two  
105 virus-associated RNAs (Figure 1A), pointing to a recombination event of two types that  
106 resulted in a hybrid. The strain is closest related to HAdV-42 (species *Human*  
107 *mastadenovirus D*) in most phylogenetic analyses except for the penton base, which has the  
108 highest sequence identity with HAdV-20 (Figure 1B). Thus, the genomic composition of  
109 strain 212 was determined as HAdV-20-42-42 concerning the sequence of the penton base,  
110 the hexon, and the fiber knob.

### 112 HAdV-20-42-42 shows low seroprevalence in human subjects

113 High levels of pre-existing anti-vector humoral immunity in vaccine target populations may  
114 hamper potential use of a novel adenoviral vector as an efficacious vaccine platform, such as  
115 found for HAdV-5-based vectors (10-12). We investigated the levels of pre-existing



116 neutralizing antibodies against HAdV-20-42-42 using a panel of serum samples ( $n=103$ )  
117 taken from a cohort of healthy >50-year-old US citizens. In line with previous findings (13),  
118 ~60% of the serum samples exhibited high levels of neutralizing activity (effective at  
119 dilutions >1:200) against HAdV-5 (Fig. 2). For HAdV-35 and HAdV-20-42-42 on the other  
120 hand only ~15% of serum samples neutralized viral activity at dilutions >200 (Fig. 2). These  
121 data indicate that the seroprevalence of HAdV-20-42-42 in this cohort was low with antibody  
122 levels comparable to that of the rare serotype HAdV-35 (species HAdV-B).

123

#### 124 **Vectorization of HAdV-20-42-42**

125 In order to study the therapeutic applicability of HAdV-20-42-42, we first generated  
126 replication-incompetent vectors expressing reporter genes  $\beta$ -galactosidase (LacZ), luciferase  
127 (Luc) or Enhanced Green Fluorescent Protein (EGFP). To do so, engineered HAdV-20-42-42  
128 genomic DNA sequences were cloned into three plasmids, called the adaptor plasmid, the  
129 intermediate plasmid, and the right-end plasmid, with overlapping regions to allow for  
130 homologous recombination events (see Figure 3A). To produce replication-incompetent  
131 reporter viruses, the E1 region of HAdV-20-42-42 was replaced with an expression cassette  
132 and a reporter gene in the adaptor plasmid. In the right-end plasmid, the E3 region was  
133 deleted to create capacity for insertion of larger transgenes. To enhance the growth in a  
134 standard producer cell line (i.e. HAdV-5 E1-complementing HEK293 cells), the native E4  
135 ORF6/7 region was exchanged with that of HAdV-5 (13-15).

136 Reconstruction of the full-length recombinant HAdV-20-42-42 vector encoding the  
137 various reporter genes was achieved by homologous recombination via co-transfection of the  
138 three plasmids into HEK293 cells. After co-transfection, the HEK293 cells were subjected to  
139 a freeze-thaw cycle to release intracellular particles. After removal of cell debris by  
140 centrifugation, the supernatant was used for a reinfection of fresh HEK293 cells. At 3 days

141 post-re-infection of the fresh HEK293 cells cytopathic effect (CPE) was observed (Figure  
142 3B) and viral progeny were successfully propagated to high titers and purified with CsCl  
143 density gradients. The reporter gene expression was detected successfully in infected cells  
144 (Figure 3C).

145

#### 146 **Characterization of HAdV-20-42-42 receptor usage**

147 Well-studied adenovirus gene therapy or vaccination vectors (e.g. HAdV-5, HAdV-26 and  
148 HAdV-35) bind their fibers to CD46, coxsackie and adenovirus receptor (CAR) or  
149 desmoglein 2 (DSG2) as high affinity receptors, while their penton bases interact with  $\alpha$ v-  
150 integrins as co-receptors for internalization (16). HAdV-20-42-42 clusters to a small group of  
151 HAdV-Ds, which have been previously shown to utilize subunits of sialic acid as primary  
152 receptors for cellular attachment and/or entry. To investigate the receptor usage, we  
153 determined the transduction capacity of HAdV-20-42-42-Luc in various cell lines, expressing  
154 or lacking CAR, sialic acid-containing glycans, DSG2, or CD46 isoforms, by measuring the  
155 luciferase levels after infection. Similar to HAdV-5, HAdV-20-42-42 efficiently transduced  
156 CHO-CAR cells, but was also able to transduce Chinese hamster ovary (CHO) cells lacking  
157 the CAR receptor albeit at a much lower efficiency (Fig. 4A), suggesting that it may also  
158 utilize other receptors.

159 Although being exploited by other HAdV-D members for infection, the presence of  
160 sialic acid on cells did not increase the transduction capacity of HAdV-20-42-42. Levels of  
161 DSG2 in TC1-DSG2 monocytes also did not affect the luciferase expression of HAdV-20-42-  
162 42 (Fig. 4A). Next, the transduction efficiency was evaluated in CHO cells expressing  
163 various isoforms of CD46 (Fig. 4B). CHO-K1 cells, which lack CD46, were poorly  
164 transduced by HAdV-20-42-42. While HAdV-5 transduced all cell lines weakly and only  
165 marginally more efficient as compared to the control cell line CHO-K1, HAdV-20-42-42

transduced CHO-K1 cells expressing all CD46 isoforms more efficiently as compared to the control cell line. Cells expressing the C2 isoform were transduced more efficiently. We recently demonstrated that HAdV-26 and 56 binds to CD46 via the hexon protein (17). Surface plasmon resonance data demonstrated that the hexon protein of HAdV-20-42-42, which belongs to the same species (D) as HAdV-26 and HAdV-5, also bound to CD46, but the hexon of HAdV-5 did not (Fig. 4 C and D, respectively). The affinity and interaction half-life were determined to be 13.5  $\mu$ M and 187 s respectively (not shown). Together, these findings indicate that the novel adenoviral vector HAdV-20-42-42 is able to bind to both CAR and CD46 receptors, primarily the C2 isoform, and that the interaction with CD46 is mediated by the hexon protein. As these receptors are present in many cell types, this warrants a broad use of the novel adenoviral vector HAdV-20-42-42 in gene therapy.

177

#### 178 **HAdV-20-42-42 vector interactions with serum and coagulation factors**

The binding of many HAdV types to human coagulation blood factor X (FX) significantly affects the transduction *in vitro* and the tropism *in vivo* following intravenous (i.v.) administration (10, 18, 19). We investigated whether the presence of FX impacts the transduction efficiency of HAdV-20-42-42. Physiological concentrations of FX were incubated with cells prior to the addition of HAdV-5, -35, or HAdV-20-42-42 luciferase vectors, and intracellular luciferase levels were measured 2 days after transduction. While HAdV-35 transduction was only marginally affected by the addition of FX, the luciferase levels of HAdV-5 and in particular of HAdV-20-42-42 were substantially increased in the presence of FX (Fig. 5A). These data show a notably higher transduction potential of HAdV-20-42-42 over HAdV-5 and HAdV-35 in human saphenous vein endothelial cells (HSVEC) in the presence of FX HSVEC were infected with HAdV-20-42-42-LacZ and HAdV-5-LacZ as a control. At all doses tested, the percentage of LacZ-positive cells was higher for HAdV-

191 20-42-42 compared to HAdV-5 (Fig. 5B). These data show that HAdV-20-42-42 was capable  
192 of efficiently transducing vascular cells in the presence of FX.

193

#### 194 **HAdV-20-42-42 biodistribution following systemic delivery *in vivo***

195 To characterize the HAdV-20-42-42 vectors *in vivo* following intravenous administration, we  
196 evaluated the biodistribution patterns of HAdV-20-42-42-Luc using a previously described  
197 mouse model (20, 21). Animals inoculated with vehicle (PBS) or HAdV-5-Luc were included  
198 as negative and positive control groups, respectively. Pretreatment with clodronate liposomes  
199 (CL+) was performed on half of the animals in order to deplete macrophages, thereby  
200 reducing possible sequestration of the adenovirus vector to the liver and allowing a more  
201 efficient evaluation of the biodistribution at the whole organism level. Two days after vector  
202 administration, the animals were imaged to visualize luciferase levels (Fig. 6A).  
203 Subsequently, the mice were sacrificed and several organs were collected for adenoviral  
204 DNA quantification (Fig. 6B).

205 In the control group of animals without CL pretreatment, HAdV-5-Luc was mainly  
206 distributed in liver and spleen at the levels of  $\sim 2.5 \times 10^5$  genome copy numbers per 100 ng  
207 total DNA, while in the group pre-treated with CL the liver and spleen distribution was  
208 higher, closer to  $\sim 5 \times 10^5$  genome copy numbers (Fig. 6). HAdV-20-42-42 on the other hand  
209 appeared to have only a spleen tropism, since luciferase activity was not detected in other  
210 organs. As expected, the total DNA copy number was significantly higher when CL was  
211 added ( $\sim 2.5 \times 10^6$ ) in comparison to the group without CL pretreatment ( $1 \times 10^5$ ).

212 In order to address the short-term organ biodistribution after administration, mice  
213 were injected intravenously with PBS, HAdV-5-LacZ and HAdV-20-42-42-LacZ and  
214 sacrificed 1 hour post i.v. delivery. The biodistribution profile of HAdV-20-42-42-LacZ was

215 with a similar pattern to that of HAdV-5-LacZ with sequestration mainly observed in liver,  
216 spleen and lungs (Fig. 6C).

217

### **HAdV-20-42-42 as a candidate vaccine vector**

The potential of HAdV-20-42-42 as a vaccine vector candidate was assessed for its ability to induce cellular immune responses against a model antigen (Luciferase, Luc) in Balb/c mice after intramuscular immunization. The vector was compared side-by-side with a benchmark vector based on HAdV-26, which has undergone clinical trials for HIV, Ebola, and recently for SARS-coronavirus-2 (22-25). Mice were immunized intramuscularly with two different doses of E1- and E3-deleted HAdV-26 vector expressing luciferase (HAdV-26-Luc) or HAdV-20-42-42-Luc. Mice were sacrificed and sampled for serum and splenocytes two weeks after the prime immunization. Cellular immune responses against the vector-encoded antigen was evaluated by Luc specific-IFN- $\gamma$  ELISPOT assay. To this end, splenocytes sampled from immunized mice were stimulated overnight with a 15mer overlapping Luc peptide pool. The antigen specific immune responses were determined by measuring the relative number of IFN- $\gamma$ -secreting cells (Fig. 7A). As expected, no Luc specific responses were detected against the empty adenovectors lacking luciferase (HAdV-26.E). Furthermore, the results show that the cellular immune responses induced by HAdV-20-42-42 were comparable to the response seen for HAdV-26 at the highest immunization dose ( $10^{10}$  VP).

For their potential utility as new adenoviral vaccine vectors, the novel HAdV-20-42-42 adenoviral vector would preferably be serologically distinct from existing adenoviral vectors currently in development as vaccine vectors, such as HAdV-26. Therefore, cross-neutralization tests were performed between the novel HAdV-20-42-42 adenoviral vector and HAdV-26. To this end, mice antisera raised against these vectors during the immunization study described above were cross-tested against both vectors in an adenovirus neutralization assay. The adenovirus neutralization assay was carried out as described previously (26). Briefly, starting from a 1:16 dilution, the sera were 2-fold serially diluted, then pre-mixed with the adenoviral vectors expressing luciferase (Luc), and subsequently incubated

243 overnight with A549 cells at a multiplicity of infection (MOI) of 500. Luciferase activity  
244 levels in infected cell lysates measured 24 hours post-infection represented vector infection  
245 efficiencies. Neutralization titers against a given vector were defined as the highest serum  
246 dilution capable of giving a 90% reduction of vector infection efficiency. The neutralization  
247 titers were arbitrarily divided into the following categories: <16 (no neutralization), 16.1 to  
248 200 (low cross-neutralization), 201 to 2,000 (cross-neutralization), and >2,001 (strong cross-  
249 neutralization).

250 The results show no major cross-neutralization between the vectors tested (Fig. 7B),  
251 but a low, one-way cross-neutralization was observed with HAdV-26 antiserum displaying a  
252 neutralization titer against HAdV-20-42-42 of 23. Thus, the new adenoviral vector HAdV-  
253 20-42-42 displayed low, if any, cross-neutralization with the human adenoviral vector  
254 HAdV-26.

255 Previous reports have demonstrated a potent inflammatory immune response against  
256 Ad vectors in the hours following i.v. administration. We investigated the levels of cytokines  
257 induced following i.v. delivery of PBS, HAdV-20-42-42-LacZ or HAdV-5-LacZ in mice.  
258 Serum samples were collected at 6 h post-i.v. administration and were tested against a mouse  
259 multiplex cytokine/chemokine panel. HAdV-20-42-42 induced higher levels of pro-  
260 inflammatory mediators and in general these were elevated above the levels observed in  
261 HAdV-5 or PBS-inoculated in 14 out of the 19 cytokine/chemokines measured (Fig. 8).  
262 Specifically, IFN $\gamma$ , IL10, IL12\_p70, IL6, KC\_GRO, TNF $\alpha$ , IL15, IL17A\_F IL27 p28\_IL30,  
263 IL-9, IP10, MCP1, MIP1a and MIP2 were robustly upregulated in HAdV-20-42-42 injected  
264 animals.

265 Taken together, these data indicate that HAdV-20-42-42 triggers a robust  
266 inflammatory and cellular immune response *in vivo* following i.v. delivery.

267

268 **DISCUSSION**

269 We present the first report on the generation of a replication-incompetent HAdV-20-42-42  
270 vector and present data on initial *in vitro* and *in vivo* characterization. Our serum  
271 neutralization studies using wild type HAdV-20-42-42 virus demonstrated that this virus  
272 displayed low seroprevalence in a random set of sera derived from healthy US subjects. Low  
273 seroprevalence has been an important criterium to select a virus for vector development, as it  
274 has been amply demonstrated that the transduction capability of the vector can be hampered  
275 in the presence of a high titer of neutralizing antibodies (27).

276 Based on these initial data we set out to generate a vector system based on HAdV-20-  
277 42-42. We created a flexible three plasmid system to support HAdV-20-42-42 vector  
278 generation, allowing for the convenient insertion of transgenes into a multiple cloning site.  
279 The wild type HAdV-20-42-42 E4ORF6 region was replaced with that of Ad5, a technique  
280 that we previously adopted for the generation of other species HAdV-D viruses including  
281 HAdV-26, HAdV-48, HAdV-49 and HAdV-56 vectors. This replacement allowed for their  
282 successful production in Ad5 E1-complementing cells such as HEK293 and PER.C6<sup>®</sup> (13,  
283 28, 29) and enabled us to manufacture high quality, high titer HAdV-20-42-42 vectors  
284 carrying diverse inserts, which paves the road for large scale clinical productions.

285 Previous studies have demonstrated that HAdV-D strains can employ CAR, CD46,  
286 sialic acid-containing glycans and  $\alpha$ v-integrins as entry receptors (16). In accordance with  
287 this, we demonstrate here that HAdV-20-42-42 utilizes CAR and CD46 as receptors.  
288 Strikingly, HAdV-20-42-42, but not HAdV-5, binds to CD46 via the hexon protein, which is  
289 far more abundant on the virus capsid as compared to the fiber (i.e. 240 trimers versus 12  
290 trimers, respectively), which can make hexon:CD46-interacting vectors novel, useful features  
291 as compared to other adenovirus-based vectors that bind to CAR or CD46 through fibers.  
292 Similar to HAdV-26 and HAdV-48, this virus interacts with blood coagulation factors (10).



293 Together with data demonstrating the high transduction efficiency of cardiovascular cells in  
294 vitro, these findings suggest that this vector is potentially well suited to develop  
295 cardiovascular gene therapy approaches although further in vivo studies are required to  
296 develop this concept in more detail since the route of delivery defines tropism, delivery and  
297 inflammatory responses.

298 In addition, the data obtained from our vaccination experiments suggest that this  
299 vector is capable of eliciting potent insert specific T-cell responses at similar levels as  
300 compared to a HAdV-26 vector. The HAdV-26 vector platform has recently been  
301 successfully used to develop a potent and safe vaccine against Ebola and this vaccine has  
302 been approved for human use by European regulatory authorities. In addition, this vector is  
303 being tested for the development of preventive vaccines against HIV, RSV and more recently  
304 SARS-CoV-2 (22, 23, 30). In preclinical tests, HAdV-26 used alone was demonstrated to  
305 induce robust humoral and cellular immunity, plus it has been well tolerated in humans while  
306 eliciting target specific immunity in phase I-III trials. We were interested to test cross-  
307 neutralization between both D viruses to assess whether subsequent use of these vectors  
308 would be a possibility. Our data demonstrate that serum from HAdV-26 does not neutralize  
309 our HAdV-20-42-42 and vice versa.

310 The induction of the potent adaptive immunity required for successful vaccination  
311 vectors is dependent on sufficient activation of the innate immune system. Vaccine vectors  
312 benefit from complement activation and the production and release of cytokines and  
313 chemokines, including IL6, TNF $\alpha$ , IFN $\gamma$ , MCP1, IP10 and MIP1, which are major players in  
314 the induction of anti-viral immune responses. HAdV-20-42-42 induced all the  
315 aforementioned mediators. These same factors may translate to AdV-associated toxicity,  
316 making HAdV-20-42-42 unsuitable for intravascular delivery however. Though direct  
317 translation of innate responses obtained in mice, which lack the CD46 receptor, towards to

318 the human situation needs caution. It has been shown that AdV vector induced innate  
319 cytokine responses are triggered largely by receptor binding (31). Non-human primates may  
320 be a better model to gain insight in the induced innate immune profiles of HAdV-20-42-42  
321 compared to mice as the latter lack the functional cellular receptor CD46. Therefore, impact  
322 assessment of the cytokine profiles on generation of adaptive immune responses as well as  
323 safety require further studies in additional species. Regarding, seroprevalence, our study was  
324 limited in its geographical distribution and age. Further studies are required to assess this in  
325 wider cohorts to fully ascertain seroprevalence. To summarize, our studies into the HAdV-  
326 20-42-42 chimera demonstrate that we have identified a promising novel adenoviral vector to  
327 pursue both gene therapy and vaccine applications and therefore warrant further preclinical  
328 and clinical studies utilizing this vector.

## 329 MATERIALS AND METHODS

### 330 Origin and sequencing of HAdV-20-42-42

331 Strain 212 was isolated in the Skåne University Hospital, Lund, Sweden in 1978 (9). To  
332 obtain the complete genome sequence, it was propagated on human alveolar epithelial cells  
333 (A549), and the intracellular viral DNA was purified from infected cells (32). The genome  
334 was sequenced using Ion Torrent next-generation sequencing at the Uppsala Genome Center  
335 of the National Genomics Infrastructure (SciLifeLab; Uppsala, Sweden). The resulting reads  
336 were normalized to a 60-times coverage using BBNorm from the BBTools suite. The  
337 normalized reads were assembled de novo using Mira v4.9.5\_2 (33), and the original  
338 sequence reads were mapped to the resulting consensus sequence using the Geneious mapper  
339 at the highest sensitivity with five iterations in Geneious 9.1.8 (34). After mapping the  
340 sequence reads to the *de novo* assembly, the final read coverage minimum was 51, the mean  
341 was 1048.4, and the read coverage's standard deviation was 274.5. The new consensus  
342 sequence was annotated based on HAdV reference strain genome annotations, using the  
343 Annotate & Predict function of Geneious.

344

### 345 Phylogenetic analysis

346 Phylogenetic analyses were conducted based on the complete genome sequence and derived  
347 amino acid sequences of the entire hexon and penton base; and also on hexon loop 1  
348 (delimited according to Yuan et al. (35)) and the fiber knob. For phylogenetic tree inference,  
349 multiple alignments were conducted using MAFFT (36), and phylogenetic calculations were  
350 performed using RAxML-NG v0.9.0 (37) based on alignments edited in trimAl v1.2 (38).  
351 Evolutionary model selection was performed using ModelTest-NG v0.1.5 (39). The  
352 robustness of the trees was determined with a non-parametric bootstrap calculation using  
353 1000 repeats. Phylogenetic trees were visualized using MEGA 7 (40), trees were rooted on

the midpoint, and bootstrap values are given as percentages if they reached 75%.  
Recombination events were analyzed using SimPlot v3.5.1 (41).

### **HAdV seroneutralization**

Serological inhibition of HAdV-20-42-42, HAdV-35 and HAdV-5 transduction was evaluated over a collection of 103 serum samples from a cohort of healthy >50-year-old US citizens. Seroneutralization assays were performed using the protocol described in Sprangers *et al.* (26). Briefly, serum samples were heat-inactivated at 56 °C for 60 min, and then twofold dilutions were performed in a 96-well tissue culture plate. The dilutions covered a range from 1/16 to 1/4096 in an end volume of 50 µl DMEM. Negative controls consisted of DMEM alone. After addition of 50 µl virus solution ( $1 \times 10^8$  VP ml<sup>-1</sup>) to each well, a cell suspension ( $10^4$  A549 cells) was added to the well to a final volume of 200 µl. Following 24 h incubation, the luciferase activity in the cells was measured using a Steady-Glo luciferase reagent system (Promega). The neutralization titers were defined as the maximum serum dilution that neutralized 90% of luciferase activity.

### **Cell lines**

HEK293 (human embryonic kidney cells: ATCC CRL-1573) were grown in Dulbecco's modified Eagle's medium (DMEM) supplemented with 10% foetal bovine serum (FBS; Gibco, UK). A549 (human lung epithelial carcinoma: ATCC CCL-185) cells were grown in RPMI-1640, supplemented with 10% FBS, 1% penicillin/streptomycin (P/S), 1% L-glutamine (Gibco) and 1% Na-Pyr (Sigma, UK). Chinese hamster ovary (CHO) cells (42), CHO-CAR (42), various CHO-CD46 cells (43) were grown as described before. TC1-DSG2 cells, a kind gift of dr. A Lieber (University of Washington, Seattle, WA, USA), were grown in RPMI supplemented with 10% FBS and 20 mM HEPES.

379

**380 Construction of replication-incompetent recombinant HAd-20-42-42 vectors**

381 The wild type HAd-20-42-42 virus was plaque purified and propagated on HEK293 cells and  
382 purified by cesium chloride (CsCl) density gradient centrifugation. From the purified virus  
383 material full genomic DNA was isolated which served as starting material for the  
384 construction of the HAdV-20-42-42 plasmids.

385

**386 HAdV-20-42-42 cloning system**

387 The HAdV-20-42-42 vector construction strategy was based on a three-plasmid system with  
388 sufficient homology between each of the plasmids to enable homologous recombination *in*  
389 *vitro* following the co-transfection in HAdV-5 E1-complementing HEK293 cells. Adapter  
390 plasmids that contain the left end of the HAdV-20-42-42 genome with E1 deletions and  
391 include either luciferase, EGFP or LacZ reporter genes, were generated first. Briefly, the  
392 adapter plasmid pAdApt20-42-42 (nt 1–461 of WT HAdV-20-42-42) contained the left  
393 inverted terminal repeat (ITR) and included an expression cassette consisting of a CMV  
394 promoter followed by a multiple cloning site, encompassing Luc, GFP or LacZ, and the SV40  
395 poly(A) signal. This plasmid also contained the wild type HAdV-20-42-42 nucleotides (nt)  
396 3361-5908 to allow homologous recombination in HEK293 cells, with the intermediate  
397 plasmid carrying the HAdV-20-42-42 genome from IVa2 to L3 genes (nt 2088 to 18494).  
398 The right-end plasmid contained the HAdV-20-42-42 genome from L3 gene to the right ITR  
399 (nt 15373 to 35187) and  
400 had a deletion for the E3 region, while the HAdV-5 E4-ORF6 replaced the HAdV-20-42-42  
401 E4-ORF6. The E3 region was deleted by PCR and standard cloning techniques exploiting a  
402 natural AscI site in the viral genome. To replace the native ORF6/7 by the homologue region  
403 of HAdV-5, three fragments were amplified by PCR. Two were designed to cover the region

404 upstream and downstream from the ORF6/7 to be replaced. A third PCR was performed to  
405 obtain the HAdV-5 ORF6/7 (HAdV-5 GenBank accession no. M73260 nt 32963–34077) and  
406 partly overlapping with the other two PCR products. These three PCR products were then  
407 subjected to fusion PCR and cloned into the plasmid backbone to obtain the final right-end  
408 plasmid.

409

#### 410 **Generation and production of HAdV-20-42-42-based adenoviral vectors**

411 Adenoviral vectors HAdV-20-42-42-LacZ, HAdV-20-42-42-Luc and HAdV-20-42-42-GFP  
412 were generated by co-transfection of E1-complementing HEK293 cells with the adaptor  
413 plasmid, intermediate plasmid and the right-end plasmid. Prior to transfection into HEK293  
414 cells, the three plasmids were digested with PacI to release the respective adenoviral vector  
415 genome fragments. The transfections were performed using Lipofectamine transfection  
416 reagent (Invitrogen; Carlsbad, CA) according to the manufacturer's instructions. After  
417 harvesting of the viral rescue transfections, the viruses were further amplified by several  
418 successive infection rounds on HEK293 cell cultures. The viruses were purified from crude  
419 viral harvests using a two-step cesium chloride (CsCl) density gradient ultracentrifugation  
420 procedure as described before (14). Viral particle (VP) titers were measured by a  
421 spectrophotometry-based procedure described previously (44).

422

#### 423 **Viral transduction assays**

424 The transduction assay was performed on 96 well tissue culture plates (Costar). HSVEC were  
425 seeded at  $1 \times 10^4$  cells/well. The following day monolayers were washed with PBS and viral  
426 vectors, either encoding the luciferase or  $\beta$ -galactosidase gene, were added at the indicated  
427 VP/cell concentrations in their corresponding media without serum. In the experiments in  
428 which blood coagulation factor FX was used, this was pre-incubated with the vector for

30 min at 37 °C prior to addition to the cells. The FX coagulation factor was purchased from Cambridge Bioscience and used at a physiological concentration of 10 µg/ml. After 3 h incubation at 37 °C, the cells were washed and fresh medium supplemented with 10% FBS was added, after which the cells were incubated for 48 h. For the readout of  $\beta$ -galactosidase gene expression, staining of the cells was performed using Galacto-Light Plus Assay Kit (Thermo Fisher Scientific). For the readout of luciferase activity, the plates were washed with PBS and the cells were lysed with 1× reporter lysis buffer (100 µl per well; Promega). Following a freeze-thaw cycle, luciferase (Luciferase assay system, Promega) measurements were performed with 20 µl of lysed cells in white opaque plates (Greiner BioOne) following the manufacturer's instructions. The BCA protein quantitation assays (Thermo Fisher Scientific) were performed with 20 µl lysed cells. The results were recorded in a Victor X multilabel plate reader (Perkin-Elmer). The transduction level was expressed as luminescence relative light units per mg of protein per well (RLU/mg). All of the assays were performed with four replicates of samples.

#### **Receptor usage assays**

Studies of receptor usage were performed using CHO cells, which were expressing (positive) or lacking (negative) for receptors of interest. The cells (CHO-CAR, CHO-sialic acid, CHO-DSG and CHO-CD46 (K1, BC1, BC2, C1 and C2) were seeded as four replicates in 96-well tissue culture plates and infected with HAdV-20-42-42-Luc or HAd5-Luc at a concentration of  $1 \times 10^4$  VP /cell. Cell cultures were incubated 3 h at 37 °C with 5% CO<sub>2</sub>. Luciferase levels were measured at 48-72 hours post-infection with Victor X Multilabel plate reader (Perkin Elmer) following the manufacturer's instructions. Luciferase transgene expression was presented as luminescence relative light units (RLU) per mg of protein. All assays were performed with four sample replicates for each experimental condition.

454

455 **Surface plasmon resonance**

456 CM5 sensor chips and amine-coupling kit were purchased from GE Healthcare. All surface  
457 plasmon resonance (SPR) experiments were performed at 25°C in 20 mM Hepes, 150 mM  
458 NaCl, and 5 mM Ca<sup>2+</sup> running buffer. Data were collected with a Biacore T200 instrument at  
459 a rate of 1 Hz. CD46 was coupled to the CM5 sensor chip by amine coupling reactions  
460 according to the manufacturer's instructions, aiming for an immobilization density of 2000 to  
461 2,500 resonance units (RU). The surface of the upstream flow cell was used as a reference  
462 and was subjected to the same coupling reaction in the absence of protein. The hexon analyte  
463 (produced as described earlier) (17) was serially diluted in running buffer to prepare a 2-fold  
464 concentration series 0.25 µM, 0.5 µM, and 1 µM, and then injected over reference and  
465 experimental biosensor surfaces for 120 sec at a flow rate of 30 µl/min. Blank samples  
466 containing only running buffer were also injected under the same conditions to allow for  
467 double referencing. After each cycle, the biosensor surface was regenerated with a 60-sec  
468 pulse of 10 mM Tris-glycine (pH 1.5) at a flow rate of 30 µl/min.

469

470 ***In vivo* biodistribution**

471 All animal experiments were fully approved by University of Edinburgh Animal Procedures  
472 and ethics committee and performed under the UK Home Office license in accordance with  
473 the UK Home Office guidelines. Immunocompetent outbred MF1 male mice (Charles River  
474 Laboratories) aged 8-10 weeks were used for the 48 hours post-injection biodistribution  
475 experiment. The animals were organized in six groups with five animals in each group,  
476 except the control (PBS) groups which had 3 animals. In order to deplete circulating  
477 macrophages and more efficiently evaluate the transit of the virus at the whole organism



level, 200  $\mu$ l of clodronate liposomes (CL) was intravenously (i.v.) administered to corresponding groups at 48 h prior to virus administration.

Treatment groups were i.v. infected with a single dose ( $1 \times 10^{11}$  VP diluted in 100  $\mu$ l PBS) of HAdV-20-42-42-Luc or HAdV-5-Luc. Matched control groups were injected with 100  $\mu$ l of PBS. At 48 hours post virus delivery, luciferase activity was imaged with the method IVIS Spectrum (CaliperLife Science, UK). Prior to the imaging procedure, 0.5 ml luciferin was injected to the mice. Animals were maintained under inhalational anesthesia (AB-G). Luciferase activity detected ranged from low (shown in blue) to high (shown in red) levels. After the imaging was completed, animals were sacrificed and their organs (liver, heart, spleen, kidney, intestine, pancreas and lungs) were collected for the quantification of the vector genomes as described before (13).

For the 1 hour post-injection time point, immunocompetent 8 week old C57BL/6J male mice (Charles River Laboratories) were i.v. infected with a single dose ( $1 \times 10^{11}$  VP diluted in 100  $\mu$ l PBS) of HAdV-20-42-42-LacZ (n=8) or HAdV-5-LacZ (n=8). Matched control groups were injected with 100  $\mu$ l of PBS (n=4). At 1 hour post virus delivery, animals were sacrificed and their organs (liver, heart, spleen, kidney, intestine, pancreas and lungs) were collected for the quantification of the vector genomes.

#### Serum cytokine analysis

Immunocompetent 8-week-old C57BL/6J male mice (Charles River Laboratories) were i.v. infected with a single dose ( $1 \times 10^{11}$  VP diluted in 100  $\mu$ l PBS) of HAdV-20-42-42-LacZ (n=8) or HAdV-5-LacZ (n=8). Matched control groups were injected with 100  $\mu$ l of PBS (n=4). At 6 hours post virus delivery, animals were sacrificed and blood was collected through cardiac puncture for serum isolation and subsequent cytokine analysis. Cytokine

502 profiles were determined from 6 h post-injection sera using a V-PLEX Mouse Cytokine 19-  
503 Plex Kit (MSD) and a MESO SECTOR s 600 machine (Meso Scale Discovery).

504

#### 505 **Mouse immunization study**

506 All animal experimentation was performed according to Dutch law and the Guidelines on the  
507 Protection of Experimental Animals published by the Council of the European Committee.  
508 Six-to-eight-week-old specific pathogen-free female Balb/c mice were purchased from  
509 Charles River and kept at the institutional animal facility under specified pathogen-free  
510 conditions. For prime immunization studies mice were immunized intramuscularly with  
511 HAdV-20-4-42 or HAdV-26 vectors ( $1 \times 10^9$  VP or  $1 \times 10^{10}$  VP per mouse) expressing Luc.  
512 Two weeks post-immunization, mice were sacrificed and the induction of Luc-specific IFN $\gamma$ -  
513 producing cells was measured by IFN $\gamma$  ELISPOT. In brief, mouse splenocytes were  
514 stimulated with 15-mer peptide pool spanning Luc (luc pool), medium (control negative) or  
515 phorbol myristate acetate (PMA; positive control).

516 Mice antisera against HAdV-20-42-42 and HAdV-26 were cross-tested against both vectors  
517 in an adenovirus neutralization assay. Starting from a 1:16 dilution, the sera were 2-fold  
518 serially diluted, as described elsewhere (26).

519

#### 520 **Statistical analysis**

521 Statistical analysis was performed with GraphPad Prism software. One-way ANOVA with  
522 the two tailed Student's t-test was used for statistical parameter comparison between different  
523 groups. The parameters of significance are indicated in each figure caption: \* $P < 0.05$ ,  
524 \*\* $P < 0.005$ , \*\*\* $P < 0.001$  and NS, not statistically significant,  $P > 0.05$ . The presented *in*  
525 *vitro* results are averaged data from at least three different experiments with four  
526 experimental replicates per condition. The *in vivo* experiments were performed with a

527 minimum of five animals per group. Errors bars represent the standard error of the mean  
528 (SEM). Statistical analyses were performed with SAS version 9.4 for Figure 6. Non-  
529 inferiority testing across dose was performed on  $\log_{10}$ -transformed data, with HAdV-26-Luc  
530 as a reference and a pre-specified margin of 0.5  $\log_{10}$ .

531

#### 532 **Data availability**

533 The HAdV-20-42-42 genome sequence was submitted to the NCBI Nucleotide database with  
534 accession number MW694832.

535 **ACKNOWLEDGMENTS**

536 The authors thank Prof. Stuart Nicklin and Nicola Britton (University of Glasgow) for kindly  
537 providing the HAdV-LacZ virus. This study was made possible by funding from FP7 Marie  
538 Curie Actions via the ADVEC consortium (grant agreement no.: 324325). This project has  
539 received funding from the European Union's Horizon 2020 research and innovation  
540 programme under grant agreement number 825670. The research of GLK and TP is  
541 supported by the National Research, Development and Innovation Office (OTKA  
542 NN128309), and that of GLK also by the János Bolyai Research Scholarship of the  
543 Hungarian Academy of Sciences. The assembly and phylogenetic calculations were  
544 performed using resources provided by KIFÜ, Hungary.

## 545 REFERENCES

- 546 1. Shirley JL, de Jong YP, Terhorst C, Herzog RW. 2020. Immune responses to viral gene therapy  
547 vectors. *Molecular Therapy* 28:709-722.
- 548 2. Singh S, Kumar R, Agrawal B. 2019. Adenoviral vector-based vaccines and gene therapies:  
549 Current status and future prospects. *Adenoviruses*:53.
- 550 3. Sun Y, Lv X, Ding P, Wang L, Sun Y, Li S, Zhang H, Gao Z. 2019. Exploring the functions of  
551 polymers in adenovirus-mediated gene delivery: Evading immune response and redirecting  
552 tropism. *Acta biomaterialia* 97:93-104.
- 553 4. Gao J, Zhang W, Ehrhardt A. 2020. Expanding the Spectrum of Adenoviral Vectors for Cancer  
554 Therapy. *Cancers* 12:1139.
- 555 5. Ismail AM, Cui T, Dommaraju K, Singh G, Dehghan S, Seto J, Shrivastava S, Fedorova NB,  
556 Gupta N, Stockwell TB. 2018. Genomic analysis of a large set of currently—and historically—  
557 important human adenovirus pathogens. *Emerging microbes & infections* 7:1-22.
- 558 6. Robinson CM, Singh G, Lee JY, Dehghan S, Rajaiya J, Liu EB, Yousuf MA, Betensky RA, Jones  
559 MS, Dyer DW, Seto D, Chodosh J. 2013. Molecular evolution of human adenoviruses. *Sci Rep*  
560 3:1812.
- 561 7. Gonzalez G, Koyanagi KO, Aoki K, Watanabe H. 2015. Interregional coevolution analysis  
562 revealing functional and structural interrelatedness between different genomic regions in  
563 human mastadenovirus D. *Journal of virology* 89:6209-6217.
- 564 8. Walsh MP, Chintakuntlawar A, Robinson CM, Madisch I, Harrach B, Hudson NR, Schnurr D,  
565 Heim A, Chodosh J, Seto D. 2009. Evidence of molecular evolution driven by recombination  
566 events influencing tropism in a novel human adenovirus that causes epidemic  
567 keratoconjunctivitis. *PloS one* 4:e5635.
- 568 9. Kaján GL, Lipiec A, Bartha D, Allard A, Arnberg N. 2018. A multigene typing system for human  
569 adenoviruses reveals a new genotype in a collection of Swedish clinical isolates. *PLoS One*  
570 13:e0209038.
- 571 10. Waddington SN, McVey JH, Bhella D, Parker AL, Barker K, Atoda H, Pink R, Buckley SM, Greig  
572 JA, Denby L, Custers J, Morita T, Francischetti IM, Monteiro RQ, Barouch DH, van Rooijen N,  
573 Napoli C, Havenga MJ, Nicklin SA, Baker AH. 2008. Adenovirus serotype 5 hexon mediates  
574 liver gene transfer. *Cell* 132:397-409.
- 575 11. Qiu Q, Xu Z, Tian J, Moitra R, Gunti S, Notkins AL, Byrnes AP. 2015. Impact of natural IgM  
576 concentration on gene therapy with adenovirus type 5 vectors. *J Virol* 89:3412-6.
- 577 12. Alonso-Padilla J, Papp T, Kaján GL, Benkő M, Havenga M, Lemckert A, Harrach B, Baker AH.  
578 2016. Development of Novel Adenoviral Vectors to Overcome Challenges Observed With  
579 HAdV-5-based Constructs. *Mol Ther* 24:6-16.
- 580 13. Duffy MR, Alonso-Padilla J, John L, Chandra N, Khan S, Ballmann MZ, Lipiec A, Heemskerk E,  
581 Custers J, Arnberg N, Havenga M, Baker AH, Lemckert A. 2018. Generation and  
582 characterization of a novel candidate gene therapy and vaccination vector based on human  
583 species D adenovirus type 56. *J Gen Virol* 99:135-147.
- 584 14. Havenga M, Vogels R, Zuijdgeest D, Radošević K, Mueller S, Sieuwerts M, Weichold F, Damen  
585 I, Kaspers J, Lemckert A, van Meerendonk M, van der Vlugt R, Holterman L, Hone D, Skeiky Y,  
586 Mintardjo R, Gillissen G, Barouch D, Sadoff J, Goudsmit J. 2006. Novel replication-  
587 incompetent adenoviral B-group vectors: high vector stability and yield in PER.C6 cells. *J Gen*  
588 *Virol* 87:2135-2143.
- 589 15. Nevels M, Spruss T, Wolf H, Dobner T. 1999. The adenovirus E4orf6 protein contributes to  
590 malignant transformation by antagonizing E1A-induced accumulation of the tumor  
591 suppressor protein p53. *Oncogene* 18:9-17.
- 592 16. Arnberg N. 2012. Adenovirus receptors: implications for targeting of viral vectors. *Trends*  
593 *Pharmacol Sci* 33:442-8.

- 594 17. Persson BD, John L, Rafie K, Strebl M, Frängsmyr L, Ballmann MZ, Mindler K, Havenga M,  
595 Lemckert A, Stehle T. 2021. Human species D adenovirus hexon capsid protein mediates cell  
596 entry through a direct interaction with CD46. *Proceedings of the National Academy of*  
597 *Sciences* 118.
- 598 18. Shayakhmetov DM, Gaggar A, Ni S, Li ZY, Lieber A. 2005. Adenovirus binding to blood factors  
599 results in liver cell infection and hepatotoxicity. *J Virol* 79:7478-91.
- 600 19. Parker AL, Waddington SN, Nicol CG, Shayakhmetov DM, Buckley SM, Denby L, Kembell-  
601 Cook G, Ni S, Lieber A, McVey JH, Nicklin SA, Baker AH. 2006. Multiple vitamin K-dependent  
602 coagulation zymogens promote adenovirus-mediated gene delivery to hepatocytes. *Blood*  
603 108:2554-61.
- 604 20. Coughlan L, Bradshaw AC, Parker AL, Robinson H, White K, Custers J, Goudsmit J, Van Rooijen  
605 N, Barouch DH, Nicklin SA, Baker AH. 2012. Ad5:Ad48 hexon hypervariable region  
606 substitutions lead to toxicity and increased inflammatory responses following intravenous  
607 delivery. *Mol Ther* 20:2268-81.
- 608 21. Bradshaw AC, Coughlan L, Miller AM, Alba R, van Rooijen N, Nicklin SA, Baker AH. 2012.  
609 Biodistribution and inflammatory profiles of novel penton and hexon double-mutant  
610 serotype 5 adenoviruses. *J Control Release* 164:394-402.
- 611 22. Milligan ID, Gibani MM, Sewell R, Clutterbuck EA, Campbell D, Plested E, Nuthall E, Voysey  
612 M, Silva-Reyes L, McElrath MJ, De Rosa SC, Frahm N, Cohen KW, Shukarev G, Orzabal N, van  
613 Duijnhoven W, Truysers C, Bachmayer N, Splinter D, Samy N, Pau MG, Schuitemaker H, Luhn  
614 K, Callendret B, Van Hoof J, Douoguih M, Ewer K, Angus B, Pollard AJ, Snape MD. 2016.  
615 Safety and Immunogenicity of Novel Adenovirus Type 26- and Modified Vaccinia Ankara-  
616 Vectored Ebola Vaccines: A Randomized Clinical Trial. *JAMA* 315:1610-23.
- 617 23. Baden LR, Karita E, Mutua G, Bekker LG, Gray G, Page-Shipp L, Walsh SR, Nyombayire J,  
618 Anzala O, Roux S, Laher F, Innes C, Seaman MS, Cohen YZ, Peter L, Frahm N, McElrath MJ,  
619 Hayes P, Swann E, Grunenberg N, Grazia-Pau M, Weijtens M, Sadoff J, Dally L, Lombardo A,  
620 Gilmour J, Cox J, Dolin R, Fast P, Barouch DH, Laufer DS, Group BIHS. 2016. Assessment of  
621 the Safety and Immunogenicity of 2 Novel Vaccine Platforms for HIV-1 Prevention: A  
622 Randomized Trial. *Ann Intern Med* 164:313-22.
- 623 24. Mercado NB, Zahn R, Wegmann F, Loos C, Chandrashekar A, Yu J, Liu J, Peter L, McMahan K,  
624 Tostanoski LH. 2020. Single-shot Ad26 vaccine protects against SARS-CoV-2 in rhesus  
625 macaques. *Nature*:1-6.
- 626 25. Poland GA, Ovsyannikova IG, Crooke SN, Kennedy RB. 2020. SARS-CoV-2 Vaccine  
627 Development: Current Status. *Mayo Clin Proc* 95:2172-2188.
- 628 26. Sprangers MC, Lakhai W, Koudstaal W, Verhoeven M, Koel BF, Vogels R, Goudsmit J,  
629 Havenga MJ, Kostense S. 2003. Quantifying adenovirus-neutralizing antibodies by luciferase  
630 transgene detection: addressing preexisting immunity to vaccine and gene therapy vectors. *J*  
631 *Clin Microbiol* 41:5046-52.
- 632 27. Sayedahmed EE, Elkishif A, Alhashimi M, Sambhara S, Mittal SK. 2020. Adenoviral Vector-  
633 Based Vaccine Platforms for Developing the Next Generation of Influenza Vaccines. *Vaccines*  
634 8:574.
- 635 28. Abbink P, Lemckert AA, Ewald BA, Lynch DM, Denholtz M, Smits S, Holterman L, Damen I,  
636 Vogels R, Thorner AR, O'Brien KL, Carville A, Mansfield KG, Goudsmit J, Havenga MJ, Barouch  
637 DH. 2007. Comparative seroprevalence and immunogenicity of six rare serotype  
638 recombinant adenovirus vaccine vectors from subgroups B and D. *J Virol* 81:4654-63.
- 639 29. Lemckert AAC, Grimbergen J, Smits S, Hartkoorn E, Holterman L, Berkhout B, Barouch DH,  
640 Vogels R, Quax P, Goudsmit J, Havenga MJE. 2006. Generation of a novel replication-  
641 incompetent adenoviral vector derived from human adenovirus type 49: manufacture on  
642 PER.C6 cells, tropism and immunogenicity. *J Gen Virol* 87:2891-2899.
- 643 30. Baden LR, Walsh SR, Seaman MS, Tucker RP, Krause KH, Patel A, Johnson JA, Kleinjan J,  
644 Yanosick KE, Perry J, Zablosky E, Abbink P, Peter L, Iampietro MJ, Cheung A, Pau MG,

- 645 Weijtens M, Goudsmit J, Swann E, Wolff M, Loblein H, Dolin R, Barouch DH. 2013. First-in-  
646 human evaluation of the safety and immunogenicity of a recombinant adenovirus serotype  
647 26 HIV-1 Env vaccine (IPCAVD 001). *J Infect Dis* 207:240-7.
- 648 31. Teigler JE, Iampietro MJ, Barouch DH. 2012. Vaccination with adenovirus serotypes 35, 26,  
649 and 48 elicits higher levels of innate cytokine responses than adenovirus serotype 5 in  
650 rhesus monkeys. *Journal of virology* 86:9590-9598.
- 651 32. Kajon AE, Erdman DD. 2007. Assessment of genetic variability among subspecies B1 human  
652 adenoviruses for molecular epidemiology studies, p 335-355, *Adenovirus methods and*  
653 *protocols*. Springer.
- 654 33. Chevreux B, Wetter T, Suhai S. Genome sequence assembly using trace signals and  
655 additional sequence information, p 45-56. *In* (ed), CiteSeer,
- 656 34. Kearse M, Moir R, Wilson A, Stones-Havas S, Cheung M, Sturrock S, Buxton S, Cooper A,  
657 Markowitz S, Duran C, Thierer T, Ashton B, Meintjes P, Drummond A. 2012. Geneious Basic:  
658 an integrated and extendable desktop software platform for the organization and analysis of  
659 sequence data. *Bioinformatics* 28:1647-9.
- 660 35. Yuan X, Qu Z, Wu X, Wang Y, Liu L, Wei F, Gao H, Shang L, Zhang H, Cui H, Zhao Y, Wu N, Tang  
661 Y, Qin L. 2009. Molecular modeling and epitopes mapping of human adenovirus type 3  
662 hexon protein. *Vaccine* 27:5103-10.
- 663 36. Katoh K, Standley DM. 2013. MAFFT multiple sequence alignment software version 7:  
664 improvements in performance and usability. *Mol Biol Evol* 30:772-80.
- 665 37. Kozlov AM, Darriba D, Flouri T, Morel B, Stamatakis A. 2019. RAXML-NG: a fast, scalable and  
666 user-friendly tool for maximum likelihood phylogenetic inference. *Bioinformatics* 35:4453-  
667 4455.
- 668 38. Capella-Gutierrez S, Silla-Martinez JM, Gabaldon T. 2009. trimAl: a tool for automated  
669 alignment trimming in large-scale phylogenetic analyses. *Bioinformatics* 25:1972-3.
- 670 39. Darriba D, Posada D, Kozlov AM, Stamatakis A, Morel B, Flouri T. 2020. ModelTest-NG: A  
671 New and Scalable Tool for the Selection of DNA and Protein Evolutionary Models. *Mol Biol*  
672 *Evol* 37:291-294.
- 673 40. Kumar S, Stecher G, Tamura K. 2016. MEGA7: Molecular Evolutionary Genetics Analysis  
674 Version 7.0 for Bigger Datasets. *Mol Biol Evol* 33:1870-4.
- 675 41. Lole KS, Bollinger RC, Paranjape RS, Gadkari D, Kulkarni SS, Novak NG, Ingersoll R, Sheppard  
676 HW, Ray SC. 1999. Full-length human immunodeficiency virus type 1 genomes from subtype  
677 C-infected seroconverters in India, with evidence of intersubtype recombination. *J Virol*  
678 73:152-60.
- 679 42. Bergelson JM, Cunningham JA, Droguett G, Kurt-Jones EA, Krithivas A, Hong JS, Horwitz MS,  
680 Crowell RL, Finberg RW. 1997. Isolation of a common receptor for Coxsackie B viruses and  
681 adenoviruses 2 and 5. *Science* 275:1320-3.
- 682 43. Liszewski MK, Atkinson JP. 1996. Membrane cofactor protein (MCP; CD46). Isoforms differ in  
683 protection against the classical pathway of complement. *J Immunol* 156:4415-21.
- 684 44. Maizel Jr JV, White DO, Scharff MD. 1968. The polypeptides of adenovirus: I. Evidence for  
685 multiple protein components in the virion and a comparison of types 2, 7A, and 12. *Virology*  
686 36:115-125.
- 687



688 **FIGURE LEGENDS**

689

690 **Figure 1. Identification of HAdV-20-42-42, a natural chimera.**

691 **A)** Yellow arrows in the genome map represent protein coding sequences, red arrows  
692 represent virus associated RNAs and brown arrows represent the inverted terminal repeats. In  
693 the SimPlot analysis, sequence identities to human adenovirus 20 and -42 are represented by  
694 red and green plots, respectively. **B)** Phylogenetic analysis of strain 212 (Umu009) based on  
695 the complete genome sequence and derived amino acid sequences of the hexon, the penton  
696 base, the hexon loop 1 and the fiber knob. *Human mastadenovirus D* reference strains are  
697 represented by their serotype- or genotype numbers.

698

699 **Figure 2. HAdV-20-42-42 shows low seroprevalence in studies with human subjects.**

700 HAdV-5, HAdV-35 and HAdV-20-42-42 seroneutralization by a cohort of healthy >50-year-  
701 old US citizens ( $n=103$  individual serum samples). The neutralization titers were arbitrarily  
702 divided into the following categories: <16 (no neutralization), 16 to 50, 50 to 200, 200 to 500,  
703 500 to 1000 and >1000.

704

705 **Figure 3. HAdV-20-42-42 vector generation and characterization.**

706 **A)** Schematic representation of the replication-incompetent HAdV-20-42-42 recombinant  
707 viral vector construction strategy with a three-plasmid system (adaptor, intermediate and  
708 right-end plasmid). Overlapping regions allowed homologous recombination events between  
709 the HAdV-20-42-42 sequences in HEK293 production cell line. E and L represent the “early”  
710 and “late” genes of the adenoviral genome, ITRs are the inverted terminal repeats at the 5’  
711 and 3’ends. **B)** CPE development in HEK293 cells upon transfection of three HAdV-20-42-  
712 42 plasmids. **C)** Verification of transgene (LacZ) expression. A549 cells were infected with



713 HAdV-20-42-42-LacZ at various MOIs (MOI was calculated based on cell count at the time  
714 of cell seeding). At 3 dpi cells were lysed and subjected to Western Blot analysis with an  
715 antibody against LacZ. The LacZ-specific bands are marked by a yellow rectangle. Lysates of  
716 a previous HAdV-20-42-42-LacZ infection were used as controls (+ ctrl A and B), while  
717 lysates of HAdV-20-42-42-GFP infected cells (- ctrl A) or uninfected cells (- ctrl B) were  
718 used as negative controls.

719

720 **Figure 4. Receptor usage of HAdV-20-42-42.**

721 **A)** Cells expressing (positive, dark gray bars) or lacking (negative, light gray bars) CAR,  
722 sialic acid-containing glycans or DSG2 receptors were infected with HAdV-20-42-42-Luc or  
723 HAdV-5-Luc as a control vector. **B)** CHO cells lacking CD46 (K1) or expressing various  
724 CD46 isoforms (BC1, BC2, C1, or C2) were infected with HAdV-20-42-42-Luc or HAdV-5-  
725 Luc as a control vector. **A, B)** One day post-infection, cells were lysed to determine  
726 intracellular luciferase activity. Luciferase activity is presented as relative light units (RLU)  
727 per milligram (mg) protein. All results represent averaged data from several times performed  
728 experiments, with four replicates for each condition. **(C, D)** Surface plasmon resonance  
729 analysis of hexon (analyte) interactions with CD46 (immobilized). **(C)** shows HAdV-20-42-  
730 42 hexon and **(D)** shows HAdV-5 interactions with CD46. Error bars are presented as  
731 standard error of the mean (SEM). Two-sample, two-tailed Student's t-tests,  $p < 0.05$  was  
732 considered statistically significant ( $p < 0.05^*$ ,  $p < 0.01^{**}$ ). Statistical significance was  
733 calculated for positive versus negative cells (**A**) or in comparison to the negative cell line K1  
734 **(B)**.

735

736 **Figure 5. Transduction efficiency of HAdV-20-42-42 in vascular cells.**

737 HAdV-20-42-42-Luc and -LacZ vectors were tested for transduction capacity in HSVEC  
738 (human saphenous vein endothelial cells). **A)** HSVEC were infected with HAdV-20-42-42-  
739 Luc or the control vectors HAdV-35-Luc and HAdV-5-Luc at various doses (1000, 5000, or  
740 10000 vp/cell) for 3 hours. Where indicated (dark gray bars), the vectors were incubated for  
741 30 min at 37°C with a physiological concentration of 10 µg/ml blood coagulation factor FX  
742 prior to addition to the cells. After 2 days, cells were lysed to measure intracellular luciferase  
743 activity, which is presented as relative light units (RLU) per milligram (mg) protein. Bars  
744 represent the means plus standard errors of the means (SEM) (error bars) for quadruplicate  
745 values. Two-sample, two-tailed Student's t-tests,  $p < 0.05$  was considered statistically  
746 significant ( $p < 0.05^*$ ,  $p < 0.01^{**}$ ). All results represent averaged data from several  
747 experiments, with four replicates for each condition. **B)** HSVEC were infected with various  
748 doses of HAdV-20-42-42-LacZ or HAdV-5-LacZ in the presence of FX. After 2 days, cells  
749 were stained for LacZ expression.

750

751 **Figure 6. Biodistribution profile of HAdV-20-42-42 shows mainly spleen tropism.**

752 Mice were pre-treated with clodronate (CL+) or untreated (CL-) and injected intravenously  
753 with HAdV-5-Luc or HAdV-20-42-42-Luc vectors. **A)** At 48 hours post virus delivery,  
754 luciferin was injected to the mice and luciferase activity was imaged with the method IVIS  
755 Spectrum, which ranged from low activity (shown in blue) to high activity (shown in red)  
756 levels. **B)** After imaging, animals were sacrificed and organs were collected to determine  
757 adenoviral genome copy numbers with qPCR. Data represent viral copy number per 100 ng  
758 of total DNA. Bars represent the means plus standard errors of the means (SEM). **C)**  
759 Biodistribution profile 1 hour after injection as determined by qPCR. Data represent viral  
760 copy number per 100 ng of total DNA. Bars represent the means plus standard errors of the  
761 means (SEM).

762

**Figure 7. Candidate vector HAdV-20-42-42 elicits strong immune response in mice.**

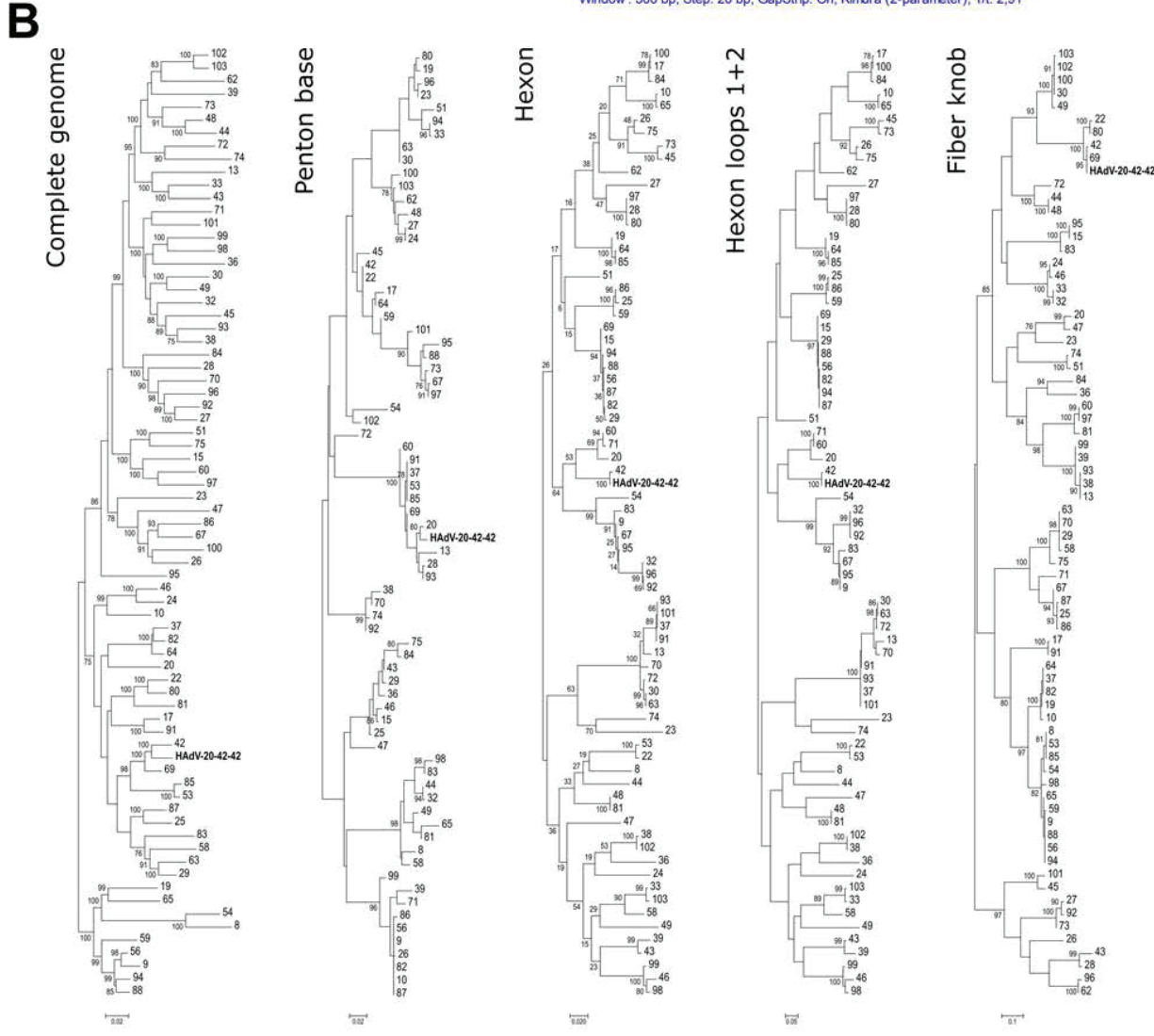
**A)** Cellular immune response in mice. Balb/C mice were immunized by intramuscular injection with HAdV-26-Luc, HAdV-20-42-42-Luc, or with HAdV-26-E that lacks a transgene. Two vector doses, i.e.  $10^9$  and  $10^{10}$  viral particles per mouse, were administered and animals were sacrificed two weeks post immunization and sampled for serum and splenocytes. Cellular immune responses against the vector-encoded antigen was evaluated by Luc specific-IFN- $\gamma$  ELISPOT assay. To this end, splenocytes were stimulated overnight with a 15mer overlapping Luc peptide pool. The antigen specific immune responses were determined by measuring the relative number of IFN- $\gamma$ -secreting cells, shown as Spot Forming Units (SFU) per million cells. Each dot represents a mouse, the bar indicates the geometric mean and the dotted line is the 95<sup>th</sup> percentile based on the medium control samples. **B)** Cross-neutralization between HAdV-20-42-42 and HAdV-26. Mice antisera against hAd20V-42-42 and HAdV-26 were cross-tested against both vectors in an adenovirus neutralization assay. Starting from a 1:16 dilution, the sera were 2-fold serially diluted, then pre-mixed with the adenoviral vectors expressing luciferase, and subsequently incubated overnight with A549 cells at MOI 500 virus particles. Luciferase activity levels in infected cell lysates measured 24 hours post-infection represented vector infection efficiencies. The neutralization titers were arbitrarily divided into the categories shown in the legend on the right.

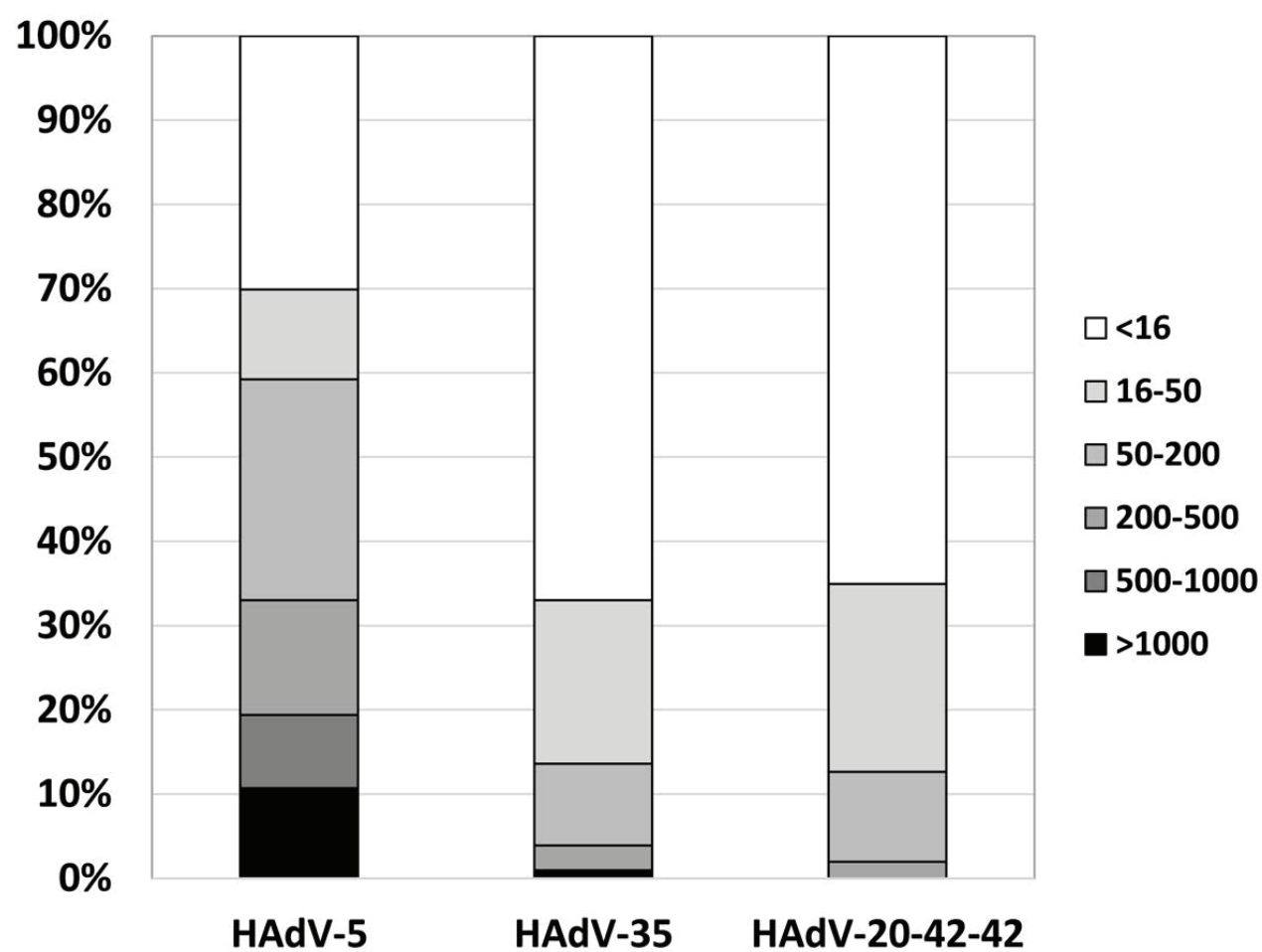
782

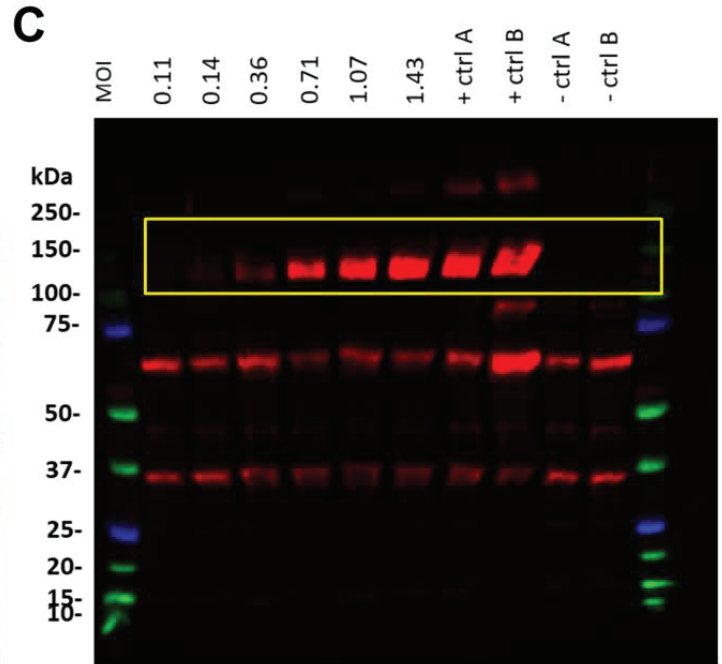
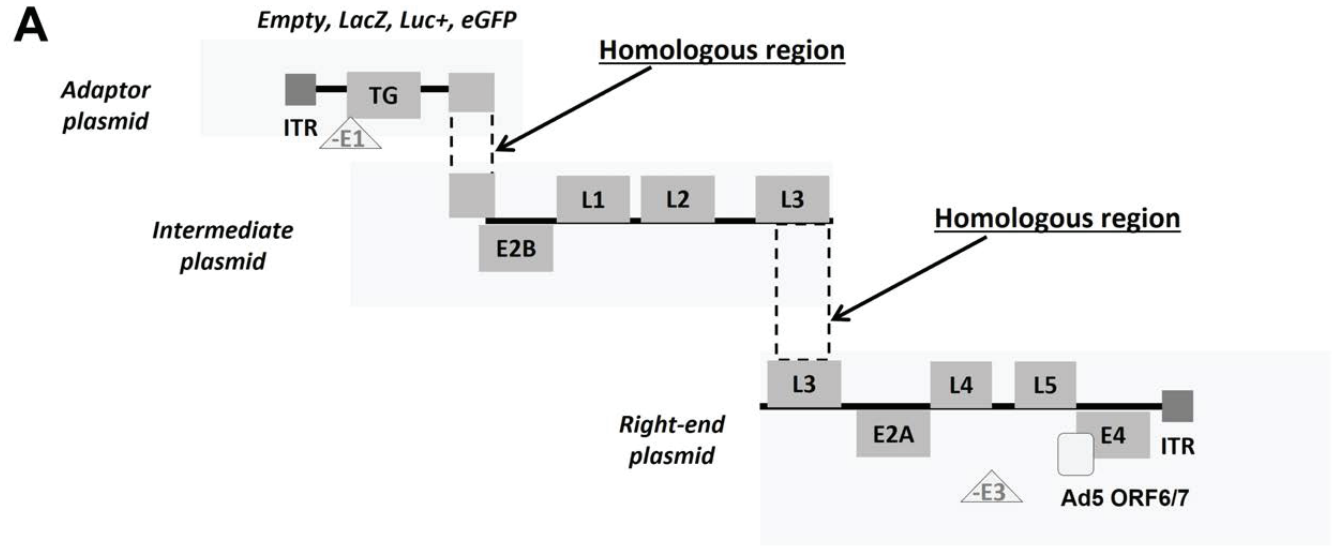
**Figure 8. Cytokine profiles upon i.v. delivery of vectors in mice.**

Cytokines were measured in blood serum samples from mice at 6 hours post-injection of PBS (control), HAdV-5-LacZ and HAdV-20-42-42-LacZ ( $1 \times 10^{11}$  VP).

785

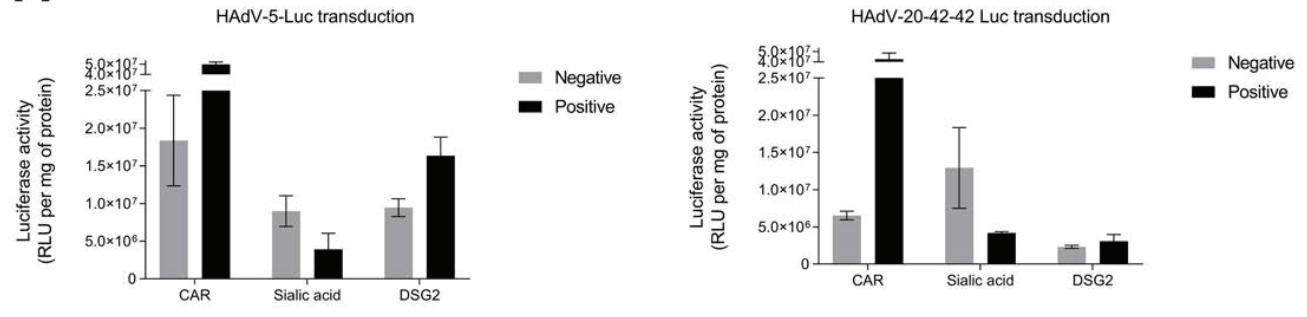




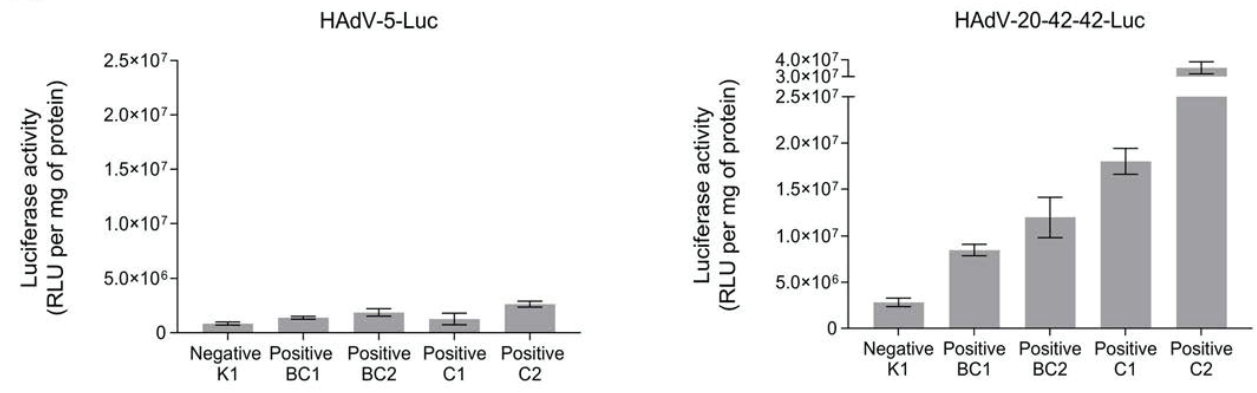




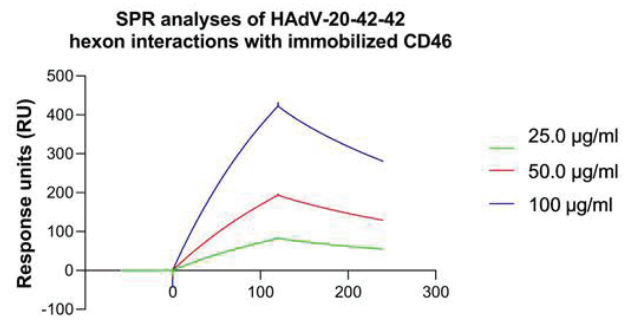
**A**



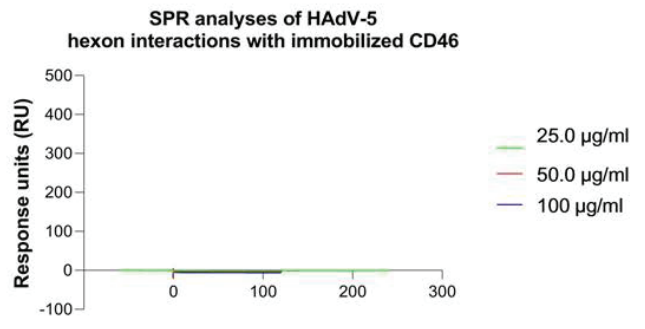
**B**

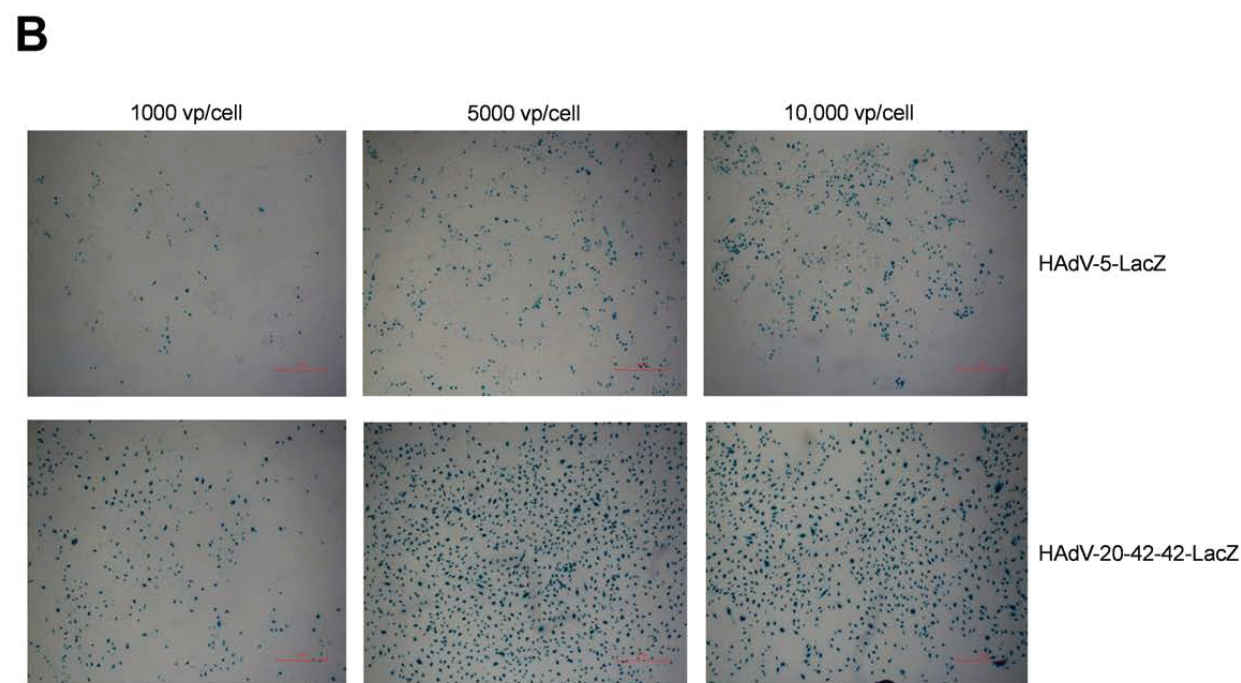
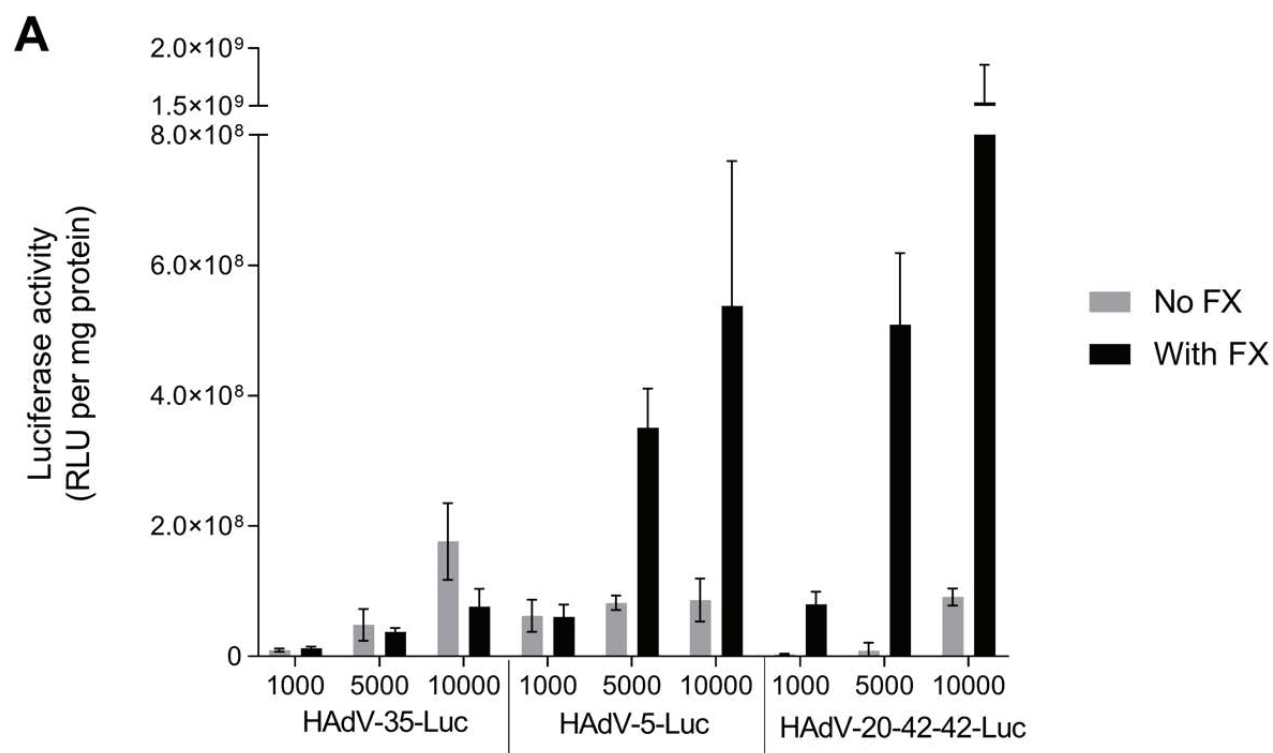


**C**

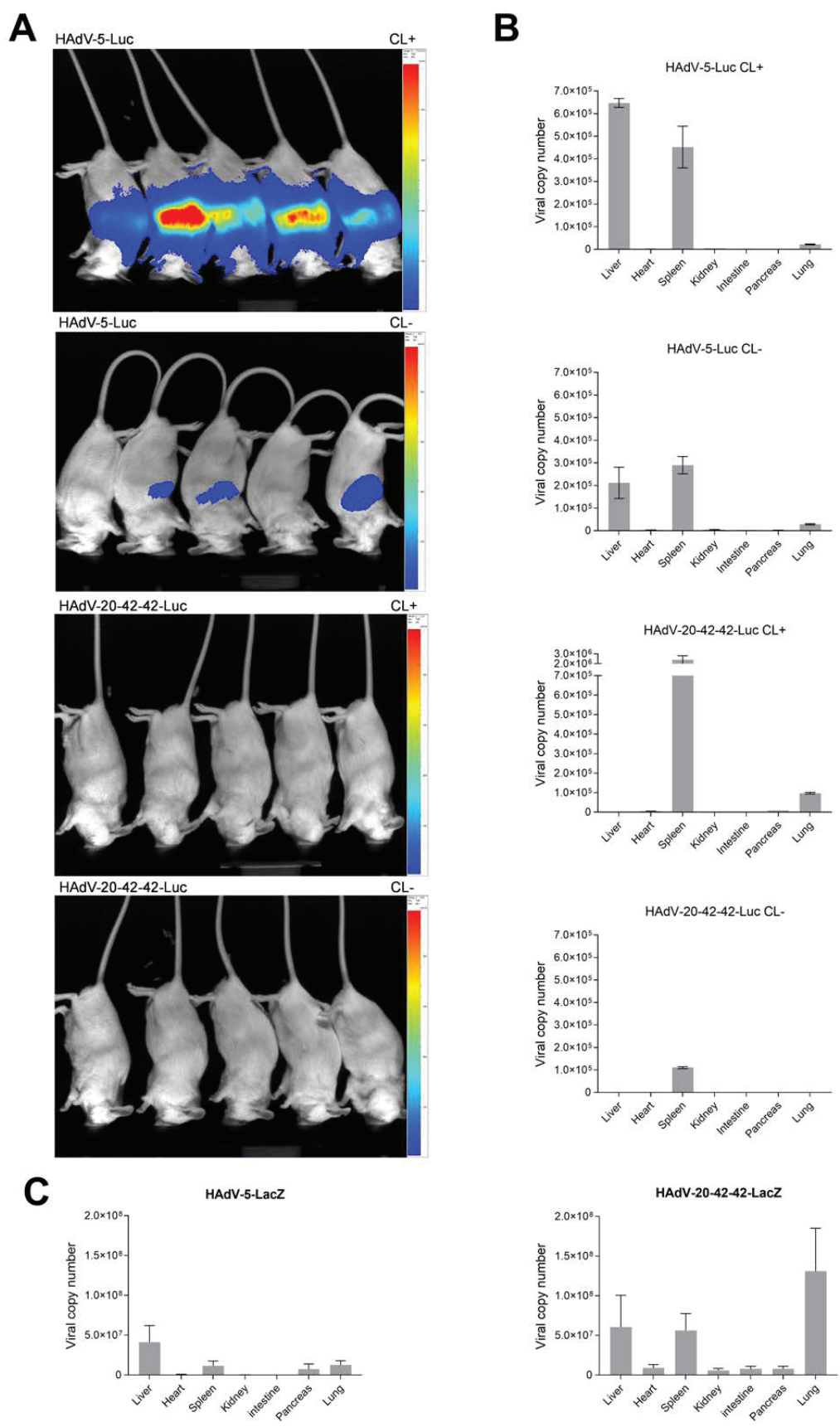


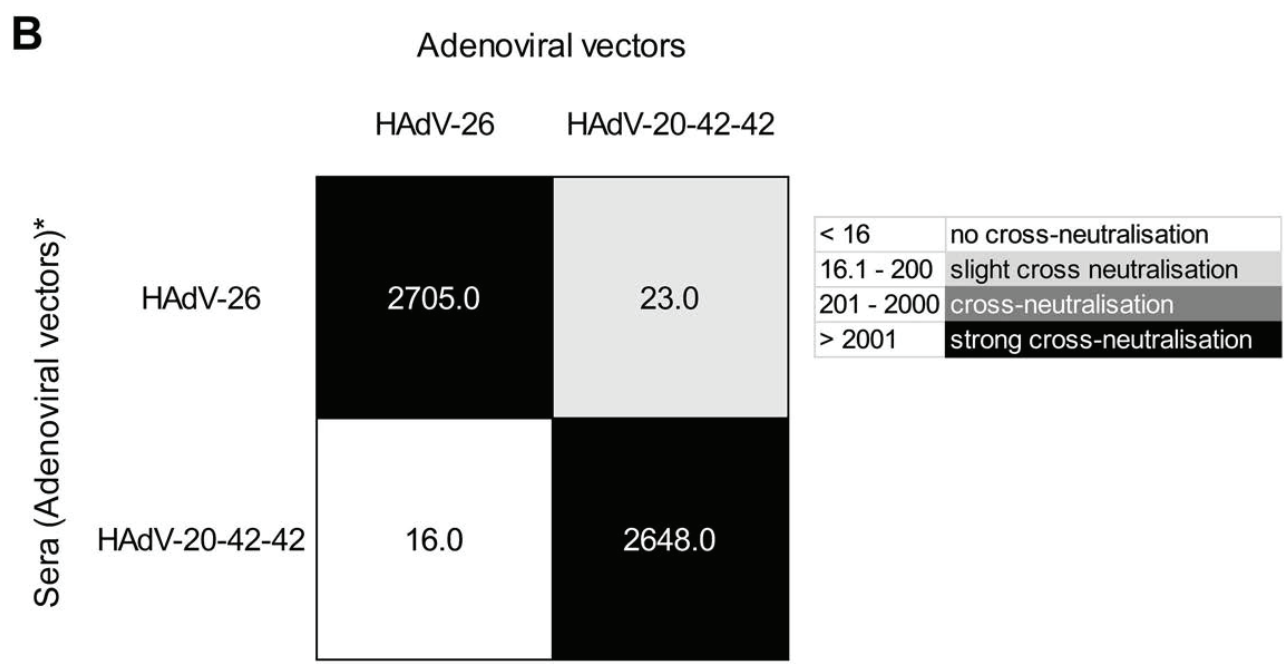
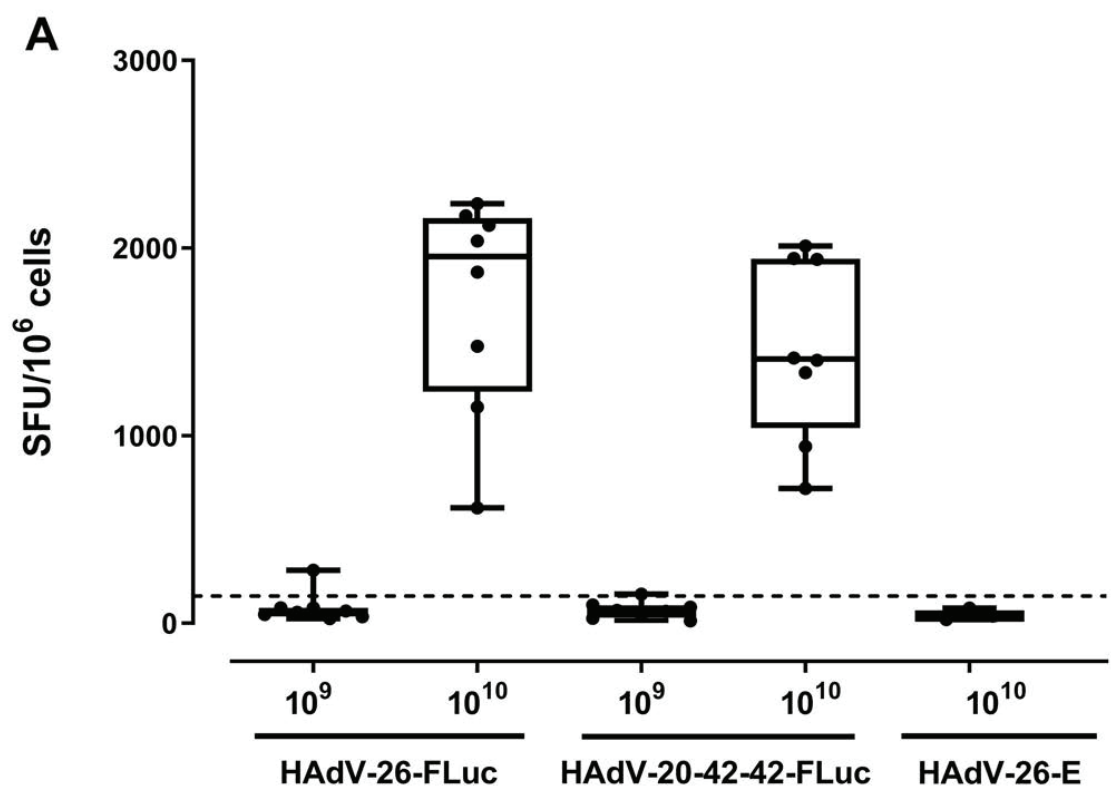
**D**



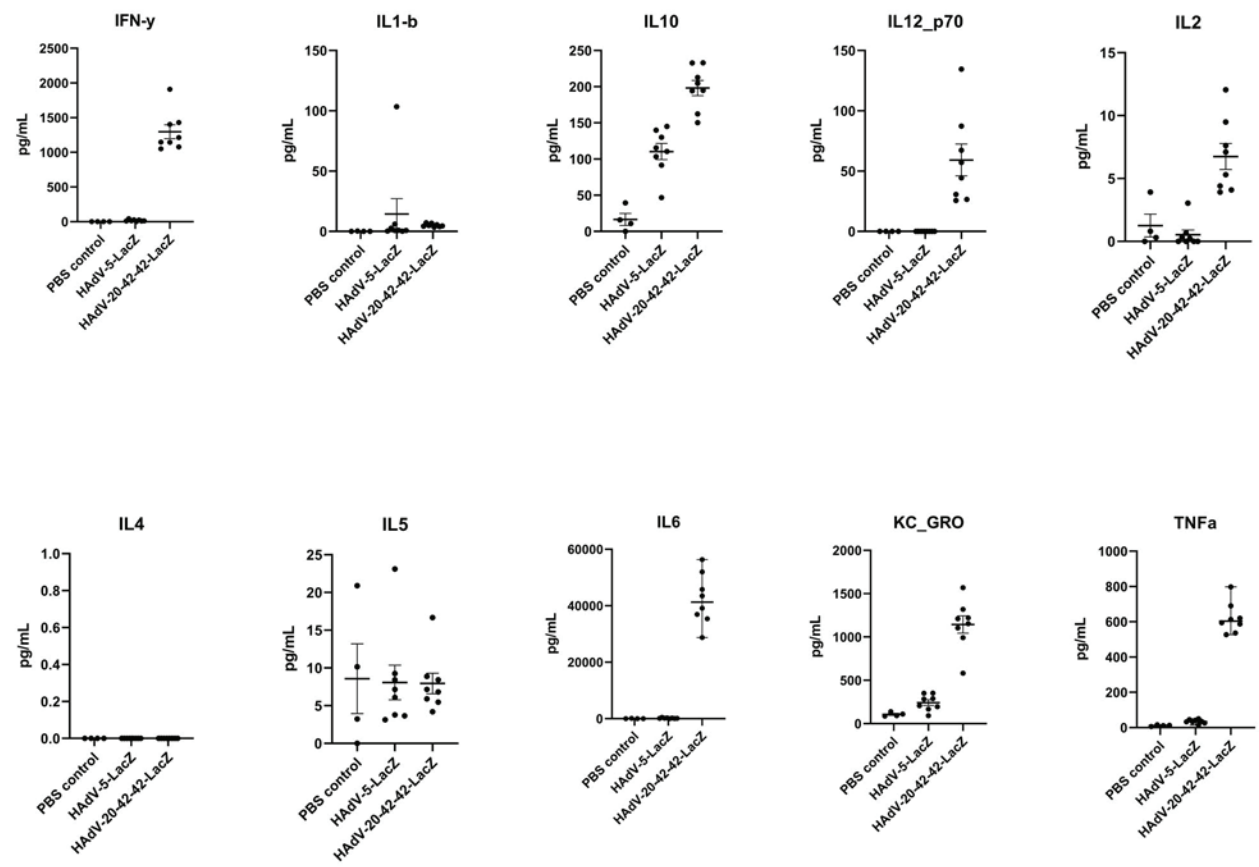








# Proinflammatory cytokines 6 hours post-injection



# Cytokine panel 6 hours post-injection

